J Math Chem (2014) 52:1497–1513
DOI 10.1007/s10910-014-0325-1

ORIGINAL PAPER

Applying structural transition theory to describe enzyme kinetics in heterogeneous systems

Jose A. C. Bispo · Carlos F. S. Bonafe · Marília L. C. Silva · Ivo H. P. Andrade · Giovani B. M. Carvalho

Received: 9 October 2013 / Accepted: 28 January 2014 / Published online: 12 February 2014

Abstract Enzyme action was investigated by assuming the occurrence of different states of enzyme-substrate affinities. These states were considered to involve enzyme species with distinct abilities to form reaction product. The results obtained showed strong agreement with the experimental data for the action of peroxidase. This approach provides a powerful tool for predicting the kinetic behavior of other enzymatic processes in conditions not described before. An additional feature of this approach is the ability to characterize processes at any enzyme-substrate concentration ratio, including high enzyme-substrate ratios and enzyme inhibition by substrate or product. This proposal can also be used in systems with heterogeneity concerning the investigated enzyme.

Keywords Enzyme kinetics · HMM and MWC models · Michaelis–Menten kinetics · Two-state model

1 Introduction

The study of enzyme action has been a very fruitful field of research ever since the pioneering work of Bohr, Henry, Michaelis–Menten and others nearly a century ago

We dedicate this paper to the memory of Professor Ines Joekes.

J. A. C. Bispo (✉) · M. L. C. Silva · I. H. P. Andrade · G. B. M. Carvalho
Departamento de Tecnologia (DTEC), Faculdade de Engenharia de Alimentos, Universidade Estadual de Feira de Santana (UEFS), CP 252/294, Feira de Santana, BA CEP 44036-900, Brazil
e-mail: jose.a.c.bispo@gmail.com

C. F. S. Bonafe
Laboratório de Termodinâmica de Proteínas, Departamento de Bioquímica, Instituto de Biologia, Universidade Estadual de Campinas (UNICAMP), Rua Monteiro Lobato 255, Campinas, SP 13083-862, Brazil

[1]. Since these initial studies, our knowledge of the mechanisms of enzyme action (activation, inhibition and modulation by allosteric factors) has expanded considerably, as has our understanding of the role of these proteins in a variety of physiological processes, including metabolic pathways, acid-basic control and oxygen transport. In the latter case, the process of oxygen transport by hemoglobin, one of most studied proteins, is considered by many to be an example of enzyme action as well as a classic case of allosteric control by ions and organic compounds involving quaternary structural modifications [2–6].

The initial studies by Michaelis and Menten [7] of a kinetic model assumed a fast step involving an association between substrate (S) and enzyme (E) to form a complex (ES), followed by a slow step in which the complex dissociated to yield product (P) and free enzyme in a unidirectional process; this kinetic analysis focused on the initial process and neglected the presence of products. Subsequent studies extended the process of modelling enzyme kinetics, with implications for microbial growth [8]. Further studies demonstrated that this model could furnish valuable information on enzyme parameters of catalysis, such as the maximum velocity of reaction (Vm) and the Michaelis–Menten constant (K_M) of the reaction, parameters that provide insights into the enzyme-substrate interaction. However, in most cases, these results were based on steady-state conditions and situations where the enzyme-substrate concentration ratios were very low [9]. The validity of the traditional model was expanded by excluding the steady-state constraint through the use of differential equation systems to explain the kinetics of the process. However, even in this case, enzyme action remained dependent on low enzyme-substrate concentration ratios [9].

To address this issue, the influence of species concentrations in the overall reaction was recently examined [10]. An additional approach to this problem was reported [11], but in this case access to the enzyme profile at a low enzyme-substrate concentration ratio involved considerations and equations that are not necessary when working with extents of reaction [12]. The proposals of Tzafriri [13] and Schnell and Maini [14] gave results compatible with those of Bispo et al. [12] but, as with other studies, the basic equations of these models used the Michaelis–Menten equation and required additional equations to introduce corrections. Since the second order nature of the differential system of equations needs to be solved in order to assess the enzyme action at any enzyme-substrate concentration ratio, all of the foregoing methods are only applicable to a starting condition in which the rate constants of the Michaelis–Menten model are needed to simulate the changes in species concentration [12].

In an attempt to overcome the shortcomings indicated above, in this report we propose a new method for investigating enzyme action based on the assumption of two enzyme structures in solution with different tendencies to bind substrate, namely, a low (L) and a high (H) tendency. This approach incorporates the classic concepts of enzyme kinetics [1,7,15] with advances in the steady-state transition involving species with heterogeneous structures and states of affinity [2,16–22]. In this regard, the classic Michaelis–Menten model has recently been extended to kinetic situations beyond the steady-state condition [9]. The time-extended Eq. (34) of Bispo et al. [9] is a true mathematical extension of the initial Michaelis–Menten and Biggs–Haldane proposition that can be obtained by using Laplace transforms. Although our previous approach introduced improvements to kinetic analysis [9], it nevertheless had some

limitations. One of these was that it did not account for situations where the substrate concentration changes with time and where the reaction product can inhibit the enzyme in a process of feedback regulation.

Specifically, we studied the kinetics of potato peroxidase (POD). Peroxidases are widely distributed in nature and consist of a family of isozymes that catalyze the same or similar reactions [23]. These enzymes act on hydrogen peroxide as an electron acceptor and oxidize a variety of donor compounds, frequently resulting in colored end-products [24]. All POD contain identical heme groups but differ in their glycoprotein composition [25]. The POD of higher plants contains the ferriprotoporphyrin III prosthetic group [26]. Peroxidase substrates, such as hydrogen peroxide and guaiacol, frequently inhibit the enzyme, depending on their concentration [27].

In the present work, we studied peroxidase activity in a heterogeneous potato extract that contained different POD species, but the approach described here can be extended to investigate the mechanisms of enzyme action under any conditions, including high enzyme-substrate concentration ratios. With appropriate adaptations, this procedure can be applied to the characterization and optimization of biotechnological processes such as microbial growth, fermentation and the association/dissociation of oligomers.

2 Materials and methods

2.1 Collection of crude enzyme

Potato was used as the source of POD. Initially, the fruit was washed in tap water, peeled and chopped into small pieces. Fifty grams of fruit was homogenized in a blender with 50 mL of 0.1 mol/L phosphate-buffered saline (1.0 mol/L NaCl), pH 6.0. The mixture was then filtered successively through Black Ribbon Filter Grade 589/1 (12–25 μm) and Grade 40 (8 μm) Whatman filter paper. The filtrate was stored at −20°C and used as a source of POD.

2.2 Determination of tetraguaiacol concentration

POD activity was assayed as described previously [28]. The substrate solution was prepared daily by mixing 0.1 mL of guaiacol, 0.1 mL of H_2O_2 (30 %) and 99.8 mL of potassium phosphate buffer (0.1 mol/L, pH 6.5), with different final concentrations of guaiacol, depending on the experiment. The substrate was mixed well by shaking vigorously for a few minutes. The reaction mixture consisted of 0.2 mL of enzyme extract and 3.3 mL of substrate solution in a quartz cuvette followed by stirring with a capillary glass rod. Peroxidase activity was measured based on the increase in absorbance at 470 nm using a spectrophotometer (Varian Cary 50 Probe). The reaction was monitored for 3 min. All of the experiments were done four times for each experimental condition and the average values were used for analysis. Enzyme activity was calculated from the change in absorbance (ΔA) at 470 nm, using the equation: $Activity\ (U/L) = \Delta A\ \ per\ min \times TV \times 10^3/\varepsilon \times SV \times PL$, where ΔA per min is the change in absorbance at 470 nm min^{-1}, TV is the total volume (3.50 mL), ε is the molar extinction of tetraguaiacol at 470 nm (2.66×10^4 L mol^{-1} cm^{-1}), SV is the volume of enzyme

solution (0.2 mL), PL is the light path length (1 cm) and 10^3 is a conversion factor (mL to L). One unit of activity was defined as the amount of enzyme that produced 1 mmol of tetraguaiacol min^{-1} under the assay conditions described here.

2.3 Determination of enzyme concentration

The POD concentration was determined spectrophotometrically (Varian Cary 50 Probe spectrophotometer) at 403 nm using an extinction coefficient (ε^{196}) of $1.02 \times 10^5\,\text{cm}^{-1}\,\text{L mol}^{-1}$ [29]. The absorbance of the solution in the absence of substrate (guaiacol) was $\varepsilon^{196} = 0.025$, which yielded an enzyme concentration of 2.45×10^{-7} mol/L.

2.4 Model description

Despite the recent extension of the Michaelis–Menten kinetic model beyond the steady-state condition [9], this proposal still has some limitations. One of these limitations is that the curve of product formation versus time, instead of being linear, as in the Michaelis–Menten model, or exponential, as in Eq. 34 of Bispo et al. [9], is actually sigmoidal or hyperbolic, as observed in Bispo et al. [12] and in the present report. In an attempt to address this limitation, improve the characterization of this model and enhance the possibility of predicting these situations, we propose an approach based on the transition between two enzyme structures of low (L) and high (H) substrate affinity in solution. These distinct affinity states involve structures with weaker or stronger enzyme-substrate interactions and the process of substrate conversion of each species (L and H) is initially assumed to be described as

$$S + E_H \overset{K_{1\text{H}}}{\rightleftarrows} E_H S \overset{K_{2H}}{\rightleftarrows} E_H + P$$
$$S + E_L \overset{K_{1\text{L}}}{\rightleftarrows} E_L S \overset{K_{2L}}{\rightleftarrows} E_L + P$$

where S is the substrate, E_L and E_H correspond, respectively, to enzyme species of low and high substrate affinity, $E_L S$ and $E_H S$ are the complex forms of these two species and P is the reaction product. The time-dependence of the enzyme concentration from each state can be given by the following exponential relationships, as in our previous reports [30,31]:

$$[E]_L(t) = \exp(w_L + k_L t) \tag{1}$$
$$[E]_H(t) = \exp(w_H + k_H t) \tag{2}$$

where t is the reaction time and w and k are the parameters that coordinate the concentration dependence of the enzyme species at each reaction time. It is important to note that since the presence of different enzyme species is assumed the proposal also contemplates heterogeneous systems that involve different enzyme activities. On the

other hand, a homogeneous system containing pure enzyme is not a guarantee of the presence of only one species since the molecule can assume different conformational states.

Assuming that the free enzyme fraction of each state of affinity can be given by

$$f_L(t) = \frac{[E]_L(t)}{[E]_L(t) + [E]_H(t)} \tag{3}$$

and

$$f_H(t) = \frac{[E]_H(t)}{[E]_L(t) + [E]_H(t)} \tag{4}$$

then it follows from Bispo et al. [30,31] that Eqs. (3) and (4) can be rewritten by introducing Eqs. (1) and (2) to obtain

$$f_L(t) = \frac{\exp(\omega_L + k_L t)}{\exp(\omega_L + k_L t) + \exp(\omega_H + k_H t)} \tag{5}$$

$$f_H(t) = \frac{\exp(\omega_H + k_H t)}{\exp(\omega_L + k_L t) + \exp(\omega_H + k_H t)} \tag{6}$$

The theoretical expression for the average product formation should be modulated by the concentration of species $[E]_L$ and $[E]_H$ in solution according to the expression

$$[P] = f_L(t)P_L + f_H(t)P_H \tag{7}$$

where P_L and P_H are the limit concentrations of product generated by species L and H, respectively. Using Eqs. (5) and (6), this can be written as

$$[P] = \frac{\exp(\omega_L + k_L t)}{\exp(\omega_L + k_L t) + \exp(\omega_H + k_H t)} P_H + \frac{\exp(\omega_H + k_H t)}{\exp(\omega_L + k_L t) + \exp(\omega_H + k_H t)} P_L \tag{8}$$

However, as in Bispo et al. [30,31], this fitting equation can be simplified to only four parameters (w_1, k_1, P_L and P_H) by dividing the numerator and denominator by $\exp(\omega_H + k_H t)$ which gives

$$[P] = \frac{\exp(\omega_1 + k_1 t)}{1 + \exp(\omega_1 + k_1 t)} P_H + \frac{1}{1 + \exp(\omega_1 + k_1 t)} P_L \tag{9}$$

where, $w_1 = w_L - w_H$ and $k_1 = k_L - k_H$

so that

$$f_H(t) = \frac{\exp(\omega_1 + k_1 P)}{1 + \exp(\omega_1 + k_1 P)} \tag{10}$$

and

$$f_L(t) = \frac{1}{1 + \exp(\omega_1 + k_1 P)} \tag{11}$$

Examination of Eq. (9) shows that the values of the parameters of this equation can be obtained by a nonlinear fit of the experimental data at each condition of substrate concentration. Although the values for w_1, k_1, P_L and P_H will be constant with respect to time, they will be substrate concentration-dependent, leading to the need for a second adjustment in order to obtain a theoretical description of these results with respect to substrate concentration and the surface plots as previously described [30,31].

From Eqs. (9) to (11) we can obtain all the parameters involved in catalysis, including species concentration, Gibbs free energy, velocities of reactions and others. For this, we start by using the extent of reaction to express the time-dependence of each species in solution for this model of reaction, as previously described in detail for the Michaelis–Menten model [9,12]:

$$[S] = c_S - x_{1L}(t) - x_{1H}(t) \tag{12}$$
$$[P] = x_{2L}(t) + x_{2H}(t) \tag{13}$$
$$[E_H] = c_{EH} - x_{1H}(t) + x_{2H}(t) \tag{14}$$
$$[E_L] = c_{EL} - x_{1L}(t) + x_{2L}(t) \tag{15}$$
$$[E_H S] = x_{1H}(t) - x_{2H}(t) \tag{16}$$
$$[E_L S] = x_{1L}(t) - x_{2L}(t) \tag{17}$$
$$c_{ET} = c_{EH} + c_{EH} \tag{18}$$

where c_S is the substrate concentration at time zero, c_{ET} is the total enzyme concentration and c_{EL} and c_{EH} are the initial enzyme concentrations in states L and H, respectively, and x represents the net extent of reaction for complex formation of species L and H, $x_{1L}(t)$ and $x_{1H}(t)$, and the respective product formation, $x_{2L}(t)$ and $x_{2H}(t)$. Since the fractions $f_L(t)$ and $f_H(t)$ are directly correlated with the amount of product formation by species $x_{2L}(t)$ and $x_{2H}(t)$, from Eqs. (7) and (13), it follows that

$$x_{2L}(t) = f_L(t)\, P(t) \tag{19}$$

and

$$x_{2H}(t) = f_H(t)\, P(t) \tag{20}$$

By applying Eqs. (14), (15), (18)–(20) to Eq. (3) we obtain

$$f_L(t) = \frac{c_{EL} - x_{1L}(t) + f_L(t)\, P(t)}{c_{ET} - x_{1L}(t) - x_{1H}(t) + P(t)} \tag{21}$$

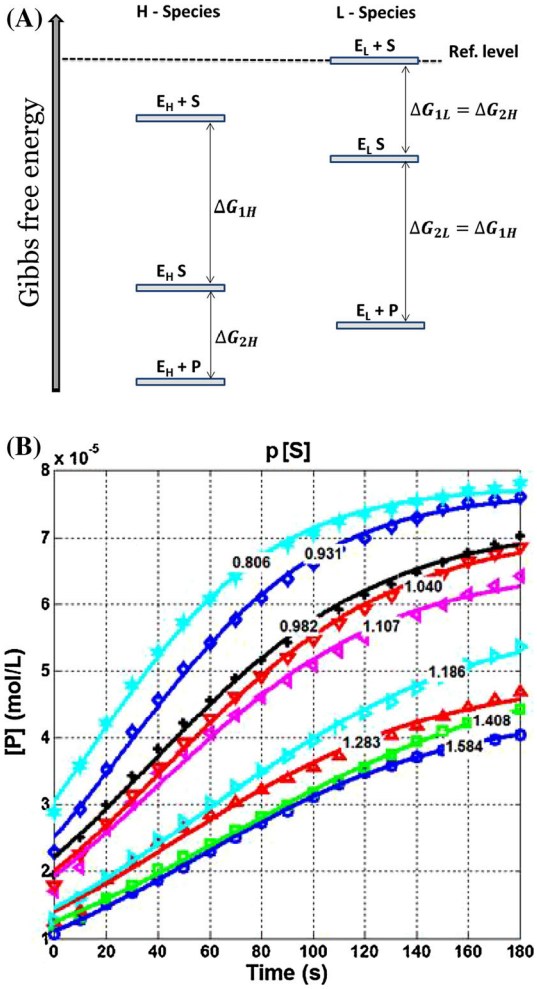

Fig. 1 **a** Gibbs free energy diagram for an enzyme reaction involving species with high (H) and low (L) substrate affinities. **b** Experimental data (symbols) for product formation versus time at different substrate potentials (p[S] $= -\log([S])$). *Lines* nonlinear fitting of the experimental data using Eq. (9) at each p[S] condition

Rewriting Eq. (21) in terms of $x_{1H}(t)$ yields

$$x_{1H}(t) = c_{ET} - \frac{c_{EL}}{f_L(t)} + \frac{f_H(t)}{f_L(t)} x_{1L}(t) \tag{22}$$

At this point, the solution of the model will depend on the energy behavior assumed by these two structures and the states of ligand affinity. Assuming that the Gibbs free energy change of complex formation is more negative for species H than for species L, as represented in Fig. 1, we can conclude that, starting from a hypothetical reference level (Fig. 1, dashed line), the absolute values of ΔG_{1H} will be higher than those for ΔG_{1L}, so with a higher substrate affinity for species H. In this model, the Gibbs free energy of product formation of the high affinity species H is identical to that for formation of the low affinity complex ($\Delta G_{2H} = \Delta G_{1L}$). An analogous

situation applies to the low affinity species ($\Delta G_{2L} = \Delta G_{1H}$). In cases involving more than two species in solution and similar energetic considerations, the model can be solved using considerations similar to those applied here. Thus, for the case where $\Delta G_{jL} = -RTln(K_{jL})$, where j is the subscript of the specified reaction (ΔG_{1L}, K_{1L}, etc), it follows from the level diagram in Fig. 1a that

$$\Delta G_{1H} + \Delta G_{2H} = \Delta G_{1L} + \Delta G_{2L} \tag{23}$$

and

$$\Delta G_{1H} = \Delta G_{2L}, \text{ as well as } \Delta G_{1L} = \Delta G_{2H} \tag{24}$$

As a consequence of Eqs. (23) and (24), we also obtain

$$K_{1H} = \frac{[E_H S]}{[E_H][S]} \tag{25}$$

and

$$K_{1L} = \frac{[E_L S]}{[E_L][S]} \tag{26}$$

such that

$$\frac{K_{1H}}{K_{1L}} = \frac{[E_H S]}{[E_H][S]} \cdot \frac{[E_L][S]}{[E_L S]},$$

And, from Eqs. (3) and (4),

$$\frac{[E_H]}{[E_L]} = \frac{f_H(t)}{f_L(t)}. \tag{27}$$

Considering that

$$\frac{K_{1H}}{K_{1L}} = \frac{[E_H S]}{[E_L S]} \cdot \frac{f_L(t)}{f_H(t)} \equiv \frac{P_H}{P_L} \tag{28}$$

it follows from Eqs. (16) and (17) that

$$\frac{[E_H S]}{[E_L S]} = \frac{f_H(t) P_H}{f_L(t) P_L} = \frac{x_{1H}(t) - x_{2H}(t)}{x_{1L}(t) - x_{2L}(t)} = \frac{x_{1H}(t) - f_H(t) P(t)}{x_{1L}(t) - f_L(t) P(t)} \tag{29}$$

Solving for $x_{1L}(t)$ in Eq. (29), we obtain

$$x_{1L}(t) = \frac{f_L(t) P_L}{f_H(t) P_H} x_{1H}(t) + \frac{(P_H - P_L)}{P_H} f_L(t) P(t) \tag{30}$$

Applying Eq. (30) to Eq. (22), a complete solution for the proposed model is reached, such that

$$x_{1H}(t) = c_{ET} - \frac{c_{EL}}{f_L(t)} + \frac{P_L}{P_H} x_{1H}(t) + \frac{(P_H - P_L)}{P_H} f_H(t) P(t) \rightarrow$$
$$x_{1H}(t) = \frac{P_H}{(P_H - P_L)} \left(c_{ET} - \frac{c_{EL}}{f_L(t)} \right) + f_H(t) P(t) \tag{31}$$

Therefore, from nonlinear adjustments of the experimental results for product formation versus reaction time and by using the previous equations, a solution for the proposed model of enzyme action is reached, with the possibility of predicting non-experimental conditions of time and substrate concentrations. Importantly, other parameters that can be obtained by this approach and that are useful for understanding the energy behavior during enzyme action are the Gibbs free energy of product formation (ΔG_{SP}) and the Gibbs free energy of structure transition (ΔG_{HL}), defined as

$$\Delta G_{SP} = -RTln\left(\frac{[P]}{[S]^4}\right) \tag{32}$$

$$\Delta G_{HL} = -RTln\left(\frac{f_L}{f_H}\right) \tag{33}$$

Here, the substrate concentration has the superscript 4 because of the stoichiometry of the peroxidase reaction in which four molecules of guaiacol (substrate) are converted into tetraguaiacol (product).

3 Results and discussion

Figure 1a shows the energy diagram corresponding to the proposed model. As can be seen, the total energy change of conversion from substrate to product is equal to the sum of both species (H and L), as discussed in the Materials and Methods section. This figure also shows that a consequence of such equivalence is that the first step involving the formation of a complex containing species H is equal to the energy change from complex to product formation of species L. This in turn means that these energy changes are reciprocal and that the assumptions that $\Delta G_{1H} + \Delta G_{2H} = \Delta G_{1L} + \Delta G_{2L}$, $\Delta G_{1H} = \Delta G_{2L}$ and $\Delta G_{2H} = \Delta G_{1L}$ are explicit in the energy diagram. Figure 1b shows the nonlinear fit (lines) of the experimental results (symbols) at each condition of substrate potential defined as $p[S] = -\log[S]$. The coefficient of determination (r^2) obtained from these nonlinear adjustments were all >0.967, indicating a good agreement between the proposed model (Eq. 9) and the experimental data.

From the fitting procedure performed for each substrate potential, the parameters of Eq. (9) were obtained (Fig. 2a–d symbols). In this case, to obtain the theoretical surface profile of the experimental data, we performed a second nonlinear fitting of the results shown in Fig. 2 (lines) that was similar to the first, but now with Eq. (9) rewritten for the substrate potential dependence (p[S]) of each parameter. The aim of this second adjustment was to obtain an analytical function able to express the

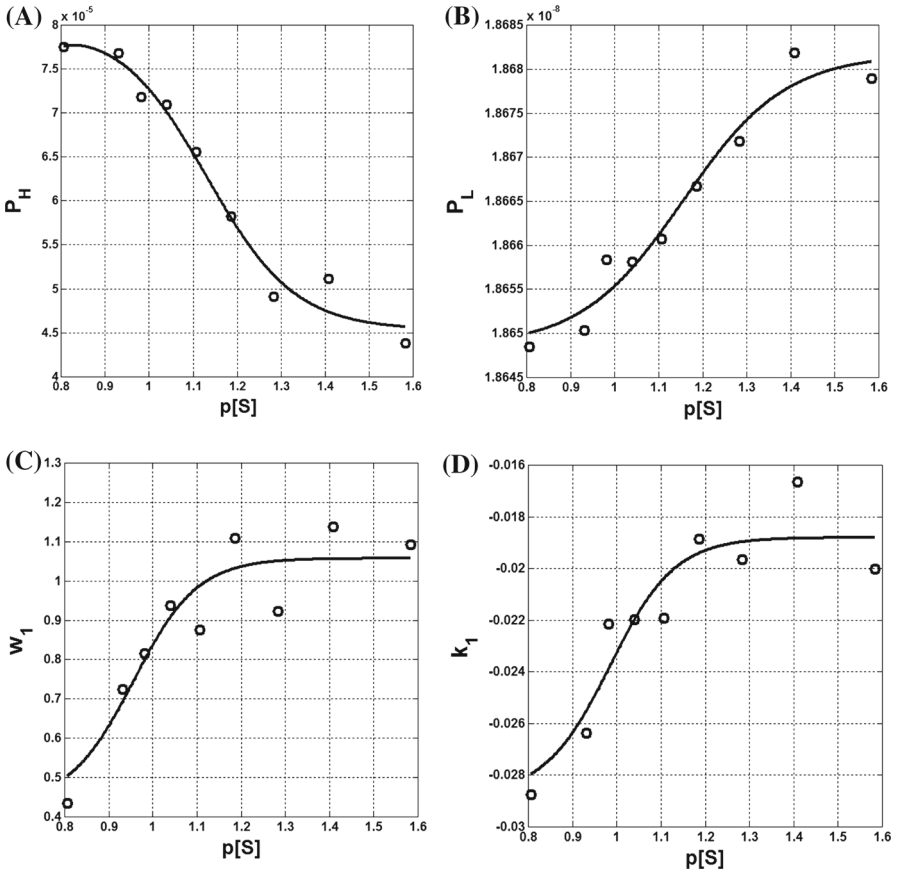

Fig. 2 Fitting parameters obtained from Fig. 1b and Eq. (9) for **a** P_H, **b** P_L, **c** w_1 and **d** k_1 at each p[S] condition. *Lines* second fitting function for each parameter

average behavior of the results gathered from the first adjustment for each parameter. This procedure allowed simulation of the theoretical predictions of the model for any condition, including those not contemplated experimentally. Consequently, it was possible to determine a surface plot of the product formation in such a way that all of the experimental data were considered to coincide with these theoretical results (Fig. 3a). Comparison of Fig. 3b with Fig. 1b revealed a slight difference between these figures, especially for the curves corresponding to p[S] values of 0.982 and 1.107, while the curves in Fig. 3b showed some deviation from the experimental data (symbols). However, since the lines in Fig. 3b were based on a combination of all the experimental data, they provided a better representation of the expected behavior for the corresponding conditions than did the symbols, particularly when a greater number of experiments was involved. Figure 3c, d show, respectively, the surface response and the cuts in this surface for changes in the degree of substrate conversion to product (α_c) for POD activity. Analysis of these panels shows that for the experimental conditions considered, the efficiency of this enzyme was very low,

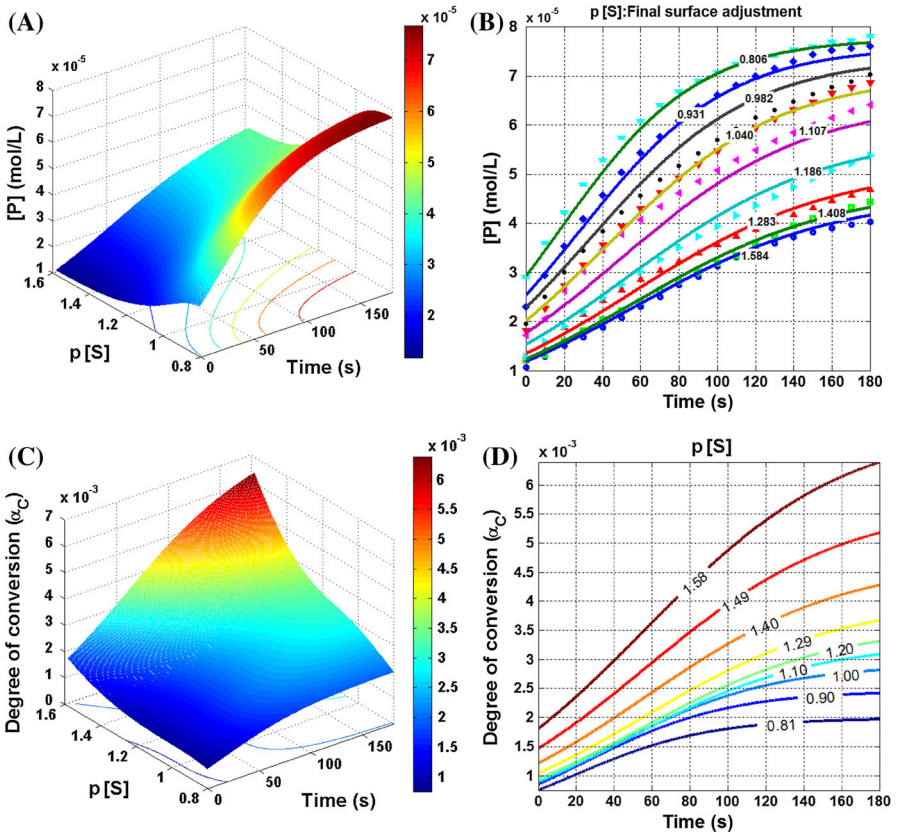

Fig. 3 **a** Surface plot of product formation as a function of substrate potential (p[S]) and reaction time. **b** Experimental data (symbols) for product formation. *Lines* final surface adjustment of the experimental data at different p[S] conditions. **c** Average degree of conversion (α_c) of substrate into product as a function of the substrate potential and reaction time. **d** Level lines of (α_c) versus reaction time at distinct substrate potentials

indicating low activity, especially at high substrate concentration or low p[S] values. This finding suggested that the high substrate concentration acted as an inhibitor.

The velocity of product formation (Vp) was obtained by the derivation of product formation with respect to time (Fig. 4). The surface plot of velocity with respect to p[S] and time is shown in Fig. 4a and the respective level curves are shown in Fig. 4b. Clearly, the curve shape differed from the hyperbolic shape normally obtained with the classic Michaelis–Menten plot (not shown). Indeed, the results in Fig. 4b demonstrate that with long reaction times there is a decrease in product formation, even at high substrate concentration, with the velocity of reaction tending to zero. According to this perspective, the time required to reach maximum velocity increases from 19 to 60 s as p[S] increases from 0.81 to 1.58. Figure 4c shows the increase in velocity with increasing substrate concentration (from high to low p[S]) that generates a region of high reaction velocities over short intervals. However, this increase was not

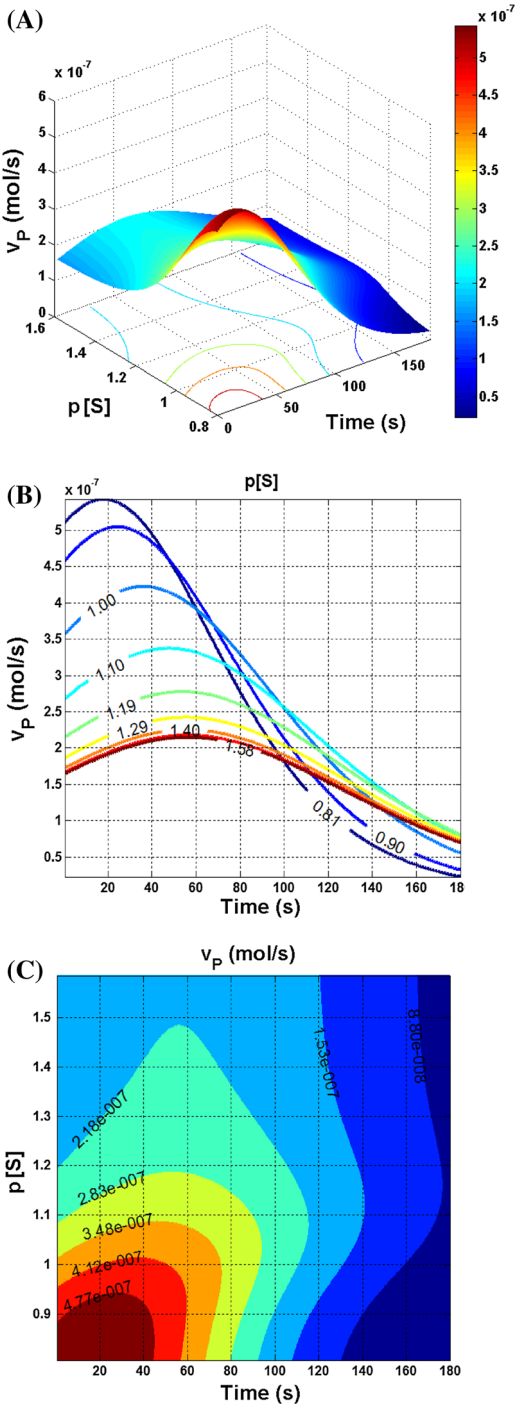

Fig. 4 **a** Surface plot of the velocity of product formation as a function of the substrate potential (p[S]) and reaction time. **b** Level lines for the velocity of product formation (V_P) versus reaction time at distinct substrate potentials. **c** Level diagram for the reaction time versus substrate potentials at distinct velocities of product formation (V_P)

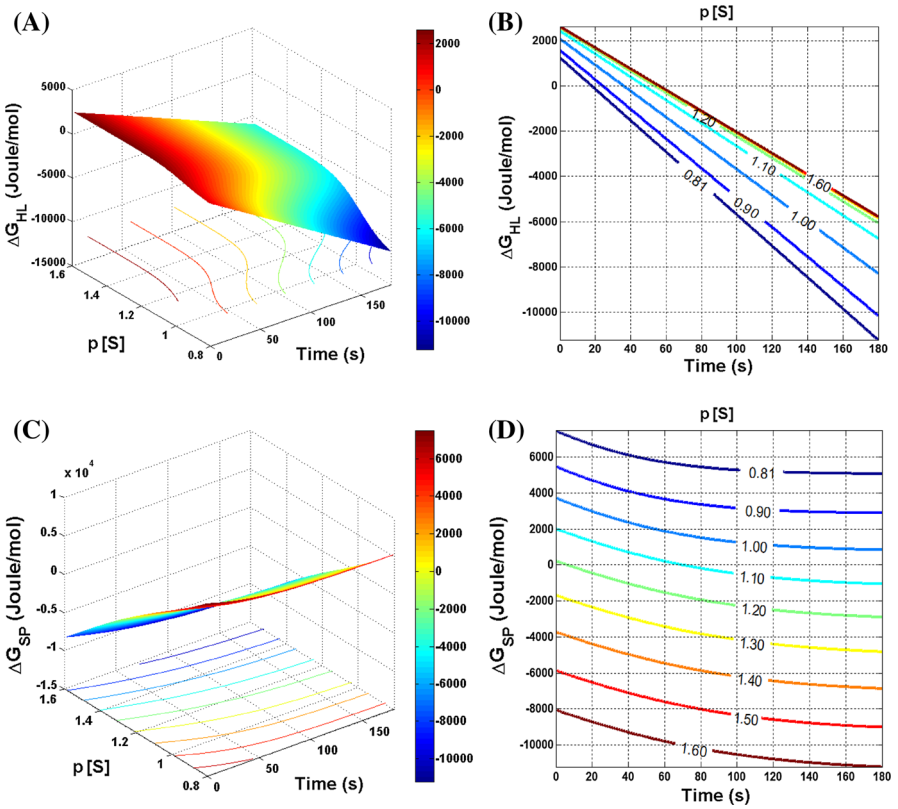

Fig. 5 **a** Surface plot of the Gibbs free energy of transition from H to L species (ΔG_{HL}) according to Eq. (33). **b** Level lines for ΔG_{HL} versus reaction time at distinct substrate potentials (p[S]). **C** Surface plot of the Gibbs free energy of product formation (ΔG_{SP}) according to Eq. (32). **d** Level lines for ΔG_{SP} versus reaction time at distinct substrate potentials (p[S])

accompanied by an increase in the degree of substrate conversion (Fig. 3d), possibly because of a higher enzyme ratio and initial substrate concentration.

Figure 5a, b shows the Gibbs free energy change of transition from species H to L calculated using Eq. (33). There was an increase in the spontaneity of the transition with time (a decrease in the values of ΔG_{HL}). The increase in the slope of ΔG_{HL} versus time with increasing substrate concentration (lower p[S]) indicated a decrease in the amount of species H in solution over time and this phenomenon was slower for lower substrate concentrations. The Gibbs free energy change of product formation (Eq. 32) is shown in Fig. 5c, d. For p[S] values <1 the process of product formation was not spontaneous ($\Delta G_{SP} > 0$) over all the time intervals observed (Fig. 5d). As p[S] increased, substrate formation became more spontaneous, thus corroborating the initial observation that the substrate acts as an inhibitor.

The profile of substrate consumption during enzyme action is shown in Fig. 6. There was no change in substrate concentration over time (Fig. 6b) and a more careful analysis showed that this was so because of the low degree of substrate conversion

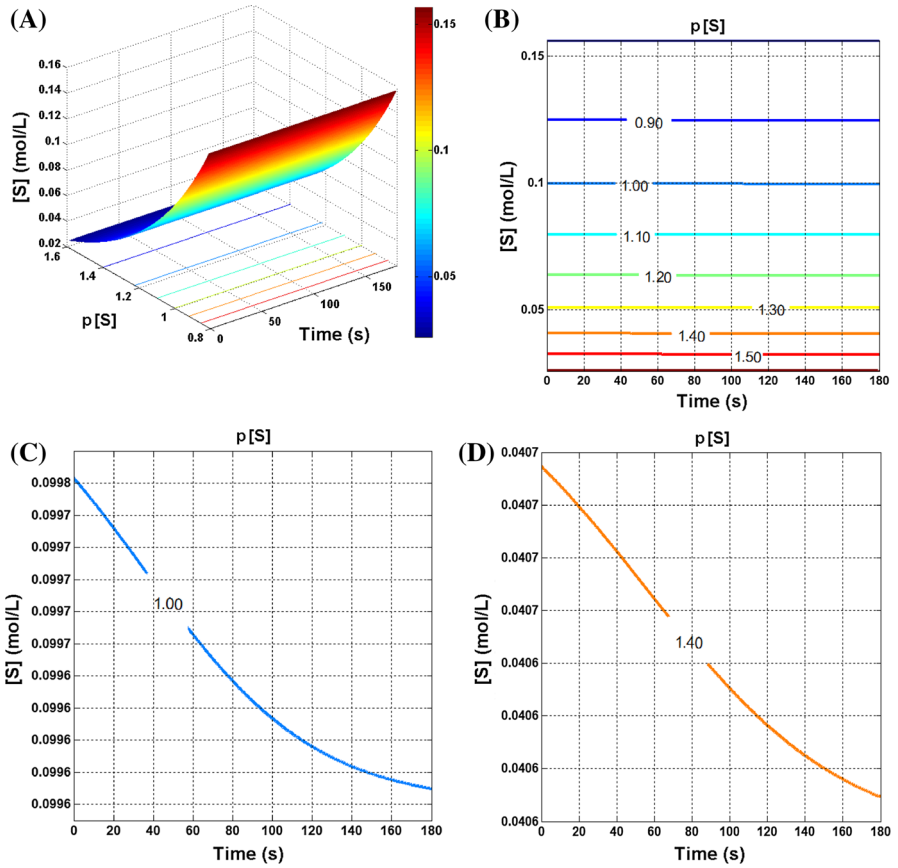

Fig. 6 **a** Surface plot of substrate concentration as a function of reaction time and substrate potential. **b** Level lines for [S] versus reaction time at distinct substrate potentials (p[S] $= -\log[S]$). **c** Expanded view of panel **b** at p[S] $= 1$. **d** Expanded view of panel **b** at p[S] $= 1.4$

observed for this enzyme. By expanding the scales of the graph in Fig. 6b for p[S] values of 1 and 1.4 it is observed that this model accounted for substrate consumption (Fig. 6c, d), a result not reported for other models in the literature. Thus, the use of Eq. (12) and the respective equations for the extent of reaction provided prompt access to these results without the need to solve differential systems of second order equations, such as typically occurs when the classic Michaelis–Menten model is assumed. The concept that the use of a low enzyme-substrate concentration ratio is a necessary constraint in order to characterize enzyme kinetics is absent in the present proposal. The exclusion of this limitation makes this approach applicable to a wide range of conditions compared to other models based on steady-state conditions and a low enzyme-substrate concentration ratio.

The present approach allows one to obtain the concentration of species from Eqs. (12) to (17). Figure 7a shows the concentration of free enzyme in solution $[E]_T$, and Fig. 7b that of species $[ES]_T$. The depletion of free enzyme and the consequent

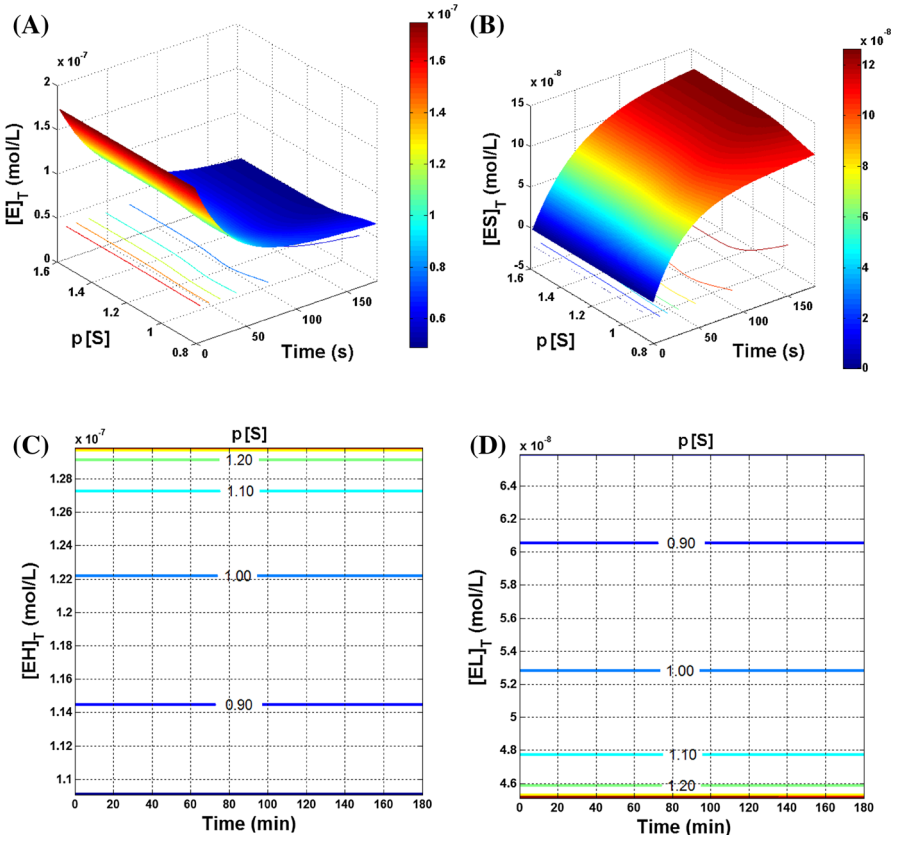

Fig. 7 **a** Surface plot of the total free enzyme concentration ($[E]_T$) as a function of the reaction time and substrate potential. **b** Surface plot of the total substrate-enzyme concentration ($[ES]_T$) as a function of the reaction time and substrate potential. **c** Level lines for the total amount of high affinity enzyme ($[EH]_T$) versus reaction time at distinct substrate potentials (p[S]). **d** Level lines for the total amount of low affinity enzyme ($[EL]_T$) versus reaction time at distinct substrate potentials (p[S])

increase in complex $[E]_T$ can be seen. The decrease in the velocity of product formation shown in Fig. 4 indicated the formation of complex species with low affinity states (L). According to the proposed model, Fig. 7c, d shows an increase in the concentration of species L and a decrease in species H, with an increase in the concentration of S (or decrease in p[S], in this case from 1.20 to 0.90), i.e., the substrate had an inhibitory effect on enzymatic activity. Moreover, the concentration of L and H species was dependent on the initial substrate concentration, which remained constant over time.

4 Conclusions

In general, the kinetic models for enzyme activity reported in the literature describe product formation with the classic constraints of steady-state conditions and high substrate concentrations for systems that are homogeneous with regard to enzyme species. Here, we have proposed an approach that does not require these constraints and have

shown that the idea that a high substrate concentration allows an approximation to the optimal conditions for enzyme action is not necessarily true, at least for some enzymes. These findings demonstrate clearly that substrate-induced inhibition should be taken into account during process optimization and that studying the mechanism of action is facilitated by this more general model. Interestingly, the Michaelis–Menten model presents limitations for describing enzyme kinetics, even for non-cooperative and monomeric enzymes with a single active site. For instance, this classic model is inadequate for describing the enzyme kinetics presented here, in which the profile of product versus time is not linear. In addition, substrate (or product) inhibition is not considered in the classic model. Thus, despite advances in the kinetic solution of the Michaelis–Menten proposal, its analytical solution is still dependent on the imposition of constraints that make it difficult to model and optimize enzyme kinetics, often to the exclusion of important experimental results related to the initial and final reaction times, for which a nonlinear profile is observed. Although the present approach needs to be validated for other systems such as allosteric enzymes and for conditions such as the presence of multiple cooperative binding sites and the presence of activators/inhibitors, the assumption of a heterogeneous systems involving the presence of two or more enzyme structures and affinity states is an interesting and powerful tool for understanding the mechanisms of enzyme action and for designing laboratory and industrial equipment and processes.

Acknowledgments The authors thank Stephen Hyslop for editing the English of the manuscript. This work was supported by Fundação de Amparo à Pesquisa do Estado da Bahia (FAPESB), Fundação de Amparo à Pesquisa do Estado de São Paulo (FAPESP), Conselho Nacional de Desenvolvimento Científico e Tecnológico (CNPq), INCT iniciative (FAPEMIG-CNPq/MCT) and Coordenação de Aperfeiçoamento de Pessoal de Nível Superior (CAPES), Brazil.

References

1. A. Cornish-Bowden, *Fundamentals of Enzyme Kinetics* (Weinheim, NY, 2012)
2. J. Monod, J. Wyman, J.P. Changeux, J. Mol. Biol. **12**, 88 (1965)
3. D.E. Koshland Jr, G. Nemethy, D. Filmer, Biochemistry **5**, 365 (1966)
4. K. Imai, T. Yonetani, J. Biol. Chem. **250**, 2227 (1975)
5. G.K. Ackers, M.L. Johnson, J. Mol. Biol. **147**, 559 (1981)
6. S.J. Edelstein, J. Mol. Biol. **257**, 737 (1996)
7. L. Michaelis, M.L. Menten, Biochem. Z **49**, 333 (1913)
8. J. Monod, Annu. Rev. Microbiol. **3**, 371 (1949)
9. J.A.C. Bispo, C.F.S. Bonafe, V.B. de Souza, J.B.A. Silva, G.B.M. Carvalho, J. Math. Chem. **49**, 1976 (2011)
10. Z. Bajzer, E.E. Strehler, Biochem. Biophys. Res. Commun. **417**, 982 (2012)
11. A.M. Bersani, G. Dell'Acqua, Math. Method. Appl. Sci. **34**, 1954 (2011)
12. J.A.C. Bispo, C.F.S. Bonafe, M.G.B. Koblitz, C.G.S. Silva, A.R. Souza, J. Math. Chem. **51**, 144 (2013)
13. A.R. Tzafriri, Bull. Math. Biol. **65**, 1111 (2003)
14. S. Schnell, P.K. Maini, Bull. Math. Biol. **62**, 483 (2000)
15. G.E. Briggs, J.B. Haldane, Biochem. J. **19**, 338 (1925)
16. G. Weber, Biochemistry **11**, 864 (1972)
17. G. Weber, Nature **300**, 603 (1982)
18. G. Weber, Proc. Natl. Acad. Sci. U. S. A. **81**, 7098 (1984)
19. G. Weber, Biochemistry **25**, 3626 (1986)
20. G. Weber, *Protein Interactions* (Chapman & Hall, New York, 1992)
21. J. Wyman Jr, Adv. Protein Chem. **4**, 407 (1948)

22. J. Wyman Jr, Adv. Protein Chem. **19**, 223 (1964)
23. L.M. Shannon, E. Kay, J.Y. Lew, J. Biol. Chem. **241**, 2166 (1966)
24. F.E. Hammer, Oxidoreductases, in *Enzymes in Food Processing*, ed. by T.W. Nagodawithana, G. Reed (Academic Press, New York, 1993), p. 233
25. T. Gaspar, C. Penel, T. Thorpe, H. Greppin, *Peroxidases, 1970–1980: A Survey of their Biochemical and Physiological Roles in Higher Plants* (Université de Genève, Centre de botanique, Geneva, 1982)
26. K.M. Mclellan, D.S. Robinson, Food Chem. **7**, 257 (1981)
27. S.M. Alencar, M.G.B. Koblitz, *Bioquímica de Alimentos* (Guanabara Koogan, Rio de Janeiro, 2008)
28. E.F. Morales-Blancas, V.E. Chandia, L. Cisneros-Zevallos, J. Food Sci. **67**, 146 (2002)
29. S. Aibara, H. Yamashita, E. Mori, M. Kato, Y. Morita, J. Biochem. (Tokyo) **92**, 531 (1982)
30. J.A.C. Bispo, C.F.S. Bonafe, I. Joekes, E.A. Martinez, G.B.M. Carvalho, D.R. Norberto, J. Phys. Chem. B **166**, 14817 (2012)
31. J.A.C. Bispo, C.M.R. Silva, C.F.S. Bonafe, D.J. Assis, Dry. Technol. **31**, 1008 (2013)